diversity

MDPI

Article

Hidden Diversity of Benthic Filamentous Cyanobacteria: Three Novel Species of Oscillatoriales Discovered in an Underexplored Urban Wetland, Eastern China

Yao Cheng [1], Yangyang Wu [2,3], Sai Zhang [4], Bangyue Zhang [5], He Zhang [2,3], Jun Zuo [2,3], Yawen Fan [1,*] and Renhui Li [1,2,3,*]

[1] College of Life Sciences and Technology, Harbin Normal University, Harbin 150025, China; wzuchengyao@163.com
[2] National and Local Loint Eneineering Research Center of Ecoloeical Treatment Technoloey for Urban WatePollution, Zheiiang Provincial Key Lab for Water Enviroment and Varie Bioloeical Resources Protection College of Life and Environmental Science, Wenzhou 325035, China; 22451335047@stu.wzu.edu.cn (Y.W.); zhanghe@wzu.edu.cn (H.Z.); jzuo@wzu.edu.cn (J.Z.)
[3] Institute for Eco-Environental Research of Sanyang Wetland, Wenzhou University, Wenzhou 325035, China
[4] Zhejiang Environmental Monitoring Engineering Co., Ltd., Hangzhou 310012, China; zs124797780@163.com
[5] The Ecological Environment Bureau of Wenzhou Pingyang, Wenzhou 325400, China; zhangbangyuemee@163.com
* Correspondence: fanyaw@163.com (Y.F.); renhui.li@wzu.edu.cn (R.L.)

Abstract

Wetlands constitute critical habitats sustaining cyanobacterial diversity. Nevertheless, taxonomic research on wetland benthic filamentous cyanobacteria is far from complete, largely limited by phenotypic plasticity and challenges in strain isolation and cultivation. To unravel the species diversity and taxonomic affiliations of epiphytic cyanobacteria in an urban wetland, cyanobacterial strains were isolated from riparian rocks of the Sanyang Wetland (Zhejiang Province) and characterized via morphological observation, 16S rRNA phylogenetic analysis and 16S–23S ITS structural comparison. Strain WZU 2025, sheathless with occasionally conical apical cells, fell into the genus *Kamptonema*. It shared less than 97.5% sequence similarity with *K. animale* and possessed distinctive ITS signatures, hereby proposed as *Kamptonema schistus* sp. nov. Strain WZU 2023, featuring colorless rigid sheaths and conical apical cells, formed a stable clade with *Microcoleus* but exhibited distinct ITS structures, and is designated *Microcoleus wenzhouensis* sp. nov. Strain WZU 2030 bears colourless rigid sheaths and trichomes mostly filled with chromatophores; it clustered reliably with known *Wilmottia* species yet differed in ITS traits, and is described as *Wilmottia sanyangensis* sp. nov. Conflicts between morphological taxonomy and molecular phylogeny reveal ambiguous intergeneric relationships within Coleofasciculaceae and Microcoleaceae. The present study expands the known diversity of Microcoleaceae and provides evidence for future taxonomic revisions of cyanobacteria. Combined with the new genus *Paludothrix* reported from this wetland in 2024, our data demonstrate that cyanobacterial diversity in Sanyang Wetland has been severely underappreciated.

Keywords: polyphasic analysis; filamentous cyanobacteria; Microcoleaceae; new species; taxonomy

Check for updates

Academic Editor: Glenn B. McGregor

Received: 9 July 2026
Revised: 5 August 2026
Accepted: 6 August 2026
Published: 7 August 2026

Copyright: © 2026 by the authors. Licensee MDPI, Basel, Switzerland. This article is an open access article distributed under the terms and conditions of the Creative Commons Attribution (CC BY) license.

1. Introduction

Wetlands are vital transitional ecosystems that connect terrestrial and aquatic environments, supporting high levels of biodiversity and providing irreplaceable ecological

functions, such as nutrient cycling, flood regulation, and habitat provision [1–3]. Located in the Ouhai District of Wenzhou, Zhejiang Province, Sanyang Wetland is a representative urban riverine wetland, encompassing a planned area of approximately 11.67 km^2. Its intricate network of 161 islands and 138 watercourses fosters heterogeneous habitats that sustain a wealth of biological resources, rendering it an ideal site for biodiversity research [4,5].

Cyanobacteria, as key primary producers, play critical roles in the cycling of materials and energy flow within wetlands, with their diversity closely linked to ecosystem stability and function. Despite their ecological significance, the taxonomy of filamentous cyanobacteria remains inadequately resolved, primarily due to their phenotypic plasticity, slow growth rates, and challenges associated with isolation and cultivation [6,7]. Traditional classification methods, which predominantly rely on morphological traits, often do not accurately represent natural evolutionary relationships, resulting in an incomplete and inconsistent taxonomic framework [8–11].

In recent decades, molecular approaches—particularly 16S rRNA phylogeny and 16S–23S ITS secondary structure analysis—have revolutionized cyanobacterial taxonomy. The polyphasic strategy, which integrates morphological, molecular, and ecological evidence, has established itself as the gold standard, resulting in significant revisions of higher-level classification [12]. In 2023, Strunecký et al. expanded cyanobacterial systematics from 8 to 20 orders, effectively resolving polyphyletic groups such as Oscillatoriales and Synechococcales [12,13].

The family Microcoleaceae (Oscillatoriales) is a diverse and ecologically significant group of filamentous cyanobacteria, with species distributed across freshwater, marine, and terrestrial habitats. The family Coleofasciculaceae was formally established following a taxonomic revision of *Microcoleus*-like taxa. Its type species, *Coleofasciculus chthonoplastes*, was originally described as *Microcoleus chthonoplastes* Thuret ex Gomont in 1892 and was later transferred to the genus *Coleofasciculus* within this newly defined family [14–16]. Many species within this family serve as pioneer colonizers of biological soil crusts, playing a crucial role in soil stability and nutrient accumulation. Since the formal establishment of the family in 2013, taxonomic studies of Microcoleaceae have progressed rapidly; however, species diversity in wetland benthic habitats remains largely underexplored. Traditional genus and species boundaries often do not align with molecular phylogenies, highlighting the necessity for further taxonomic revisions [17,18].

This study investigated epilithic benthic cyanobacteria on riparian rocks of Sanyang Wetland to fill the knowledge gap concerning wetland-dwelling *Microcoleus*-like taxa. A polyphasic approach integrating morphological observation, 16S rRNA-based phylogeny, and 16S–23S ITS secondary structure analysis was applied to clarify their diversity and taxonomic placement [19–21]. Three novel cyanobacterial species are proposed based on integrated evidence. On the basis of morphological traits, 16S rRNA gene sequence similarities to reference strains belonging to *Kamptonema*, *Microcoleus*, and *Wilmottia*, as well as divergent ITS structures, the strains isolated in the present study are designated as three new species: *K. schistus* sp. nov., *M. wenzhouensis* sp. nov., and *W. sanyangensis* sp. nov. [11,15,20–23]. Morphological–molecular phylogenetic incongruence indicated unresolved intergeneric relationships within the families Microcoleaceae and Coleofasciculaceae in urban wetland environments. The outcomes of the present study improve our knowledge of wetland cyanobacterial diversity and provide fundamental data for the taxonomic revision of Microcoleaceae and Coleofasciculaceae.

2. Materials and Methods

2.1. Strain Collection and Cultivation

Field sampling was conducted in October 2023 at the Sanyang Wetland, Zhejiang Province, China (120°43′ E, 29°57′ N) (Figure 1). Visible cyanobacterial mats on riparian rock surfaces were scraped using a soil core sampler and placed into sterile Petri dishes or sealed plastic bags. All samples were wrapped with Parafilm, kept in an icebox, and transported to the laboratory immediately for strain isolation. Given that the samples were obtained from riparian rocks, aggregated cyanobacterial colonies were first gently dissociated and homogenized. After separation of thalli and filaments, unialgal strains were isolated using the capillary isolation method and the solid agar plate method.

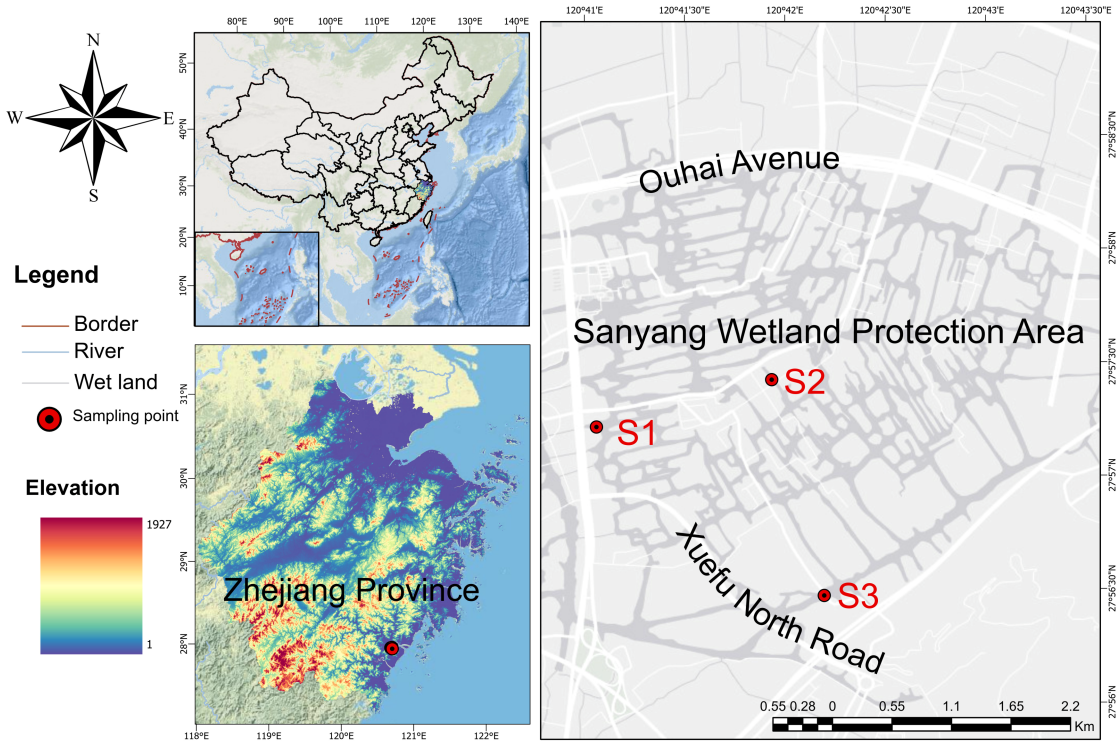


Figure 1. Sanyang Wetland in Zhejiang Province, China, with the sampling site marked on the map (S1, S2, S3).

For capillary isolation, fine glass capillaries fabricated from Pasteur pipettes were used to pick individual filaments or single cells under an inverted microscope (Olympus CKX31,Olympus Corporation, Tokyo, Japan) at 40× magnification. Field-collected samples were repeatedly rinsed with sterile CT medium and cultured in 24-well plates [24]. After unialgal growth was observed, isolates were transferred to screw-capped tubes with 10 mL sterile CT medium for routine preservation. For the plate isolation approach, CT medium was solidified using 3% (*w*/*v*) agar. Diluted cyanobacterial suspensions were spread evenly on agar plates and incubated under illumination. Following 4–6 weeks of cultivation, single filaments were picked microscopically together with adjacent agar and aseptically transferred into screw-capped tubes filled with 10 mL sterile CT medium. All unialgal cultures were incubated at 25 °C under a 12 h:12 h light/dark photoperiod with a light intensity of 30 µmol photons/(m^2·s). Subcultivation was performed at intervals of 1–2 months. The purified strains were deposited in the Algae Culture Collection of the College of Life and Environmental Sciences, Wenzhou University, under the accession numbers WZU 2023, WZU 2025, and WZU 2030. The NCBI accession numbers for the 16S–23S rRNA gene sequences of the strains are as follows: (PZ783779, PZ783778, PZ782710-PZ782711).

2.2. Morphological Characterization

When sufficient biomass was obtained, 1 mL of axenic algal suspension was aseptically sampled and diluted. Diluted suspensions were mounted on glass slides for morphological observation of live material under a LEICA DM2000 LED light microscope (Wetzlar, Germany) fitted with a LEICA DMC 5400 digital camera for micrograph capture. Micrographs were processed via Leica Application Suite X v3.7.4, and vegetative cell traits of filamentous cyanobacteria were documented at 1000× magnification. Morphometric parameters (vegetative cell width and length) were quantified from at least 60 individual filaments.

For transmission electron microscopy (TEM), roughly 100 mg cyanobacterial biomass was pelleted via centrifugation at 5000 rpm for 5 min. Pellets were prefixed in 0.1 mol/L glutaraldehyde phosphate buffer (pH 7.2) at 4 °C for 72 h, then repeatedly washed with the same buffer. Post-fixation was carried out with 1% osmium tetroxide at ambient temperature for 2 h. Following thorough buffer rinsing, samples underwent serial ethanol dehydration (30%, 50%, 70%, 90%, 100%) and embedding in Spurr's resin. Ultrathin resin sections were stained with 2% uranyl acetate and lead citrate, then imaged with an HT7700 transmission electron microscope (HITACHI, Hitachi-shi, Japan) operating at 80 kV.

2.3. DNA Extraction, PCR Amplification, and Sequencing

Genomic DNA of cyanobacterial isolates was extracted via a modified cetyltrimethylammonium bromide (CTAB) protocol [25]. The 16S–23S rRNA internal transcribed spacer (ITS) region was amplified with primer pair PA (The primers are cyanobacteria-specific primers) (5′-AGAGTTTGATCCTGGCTCAG-3′) and B23s 2(5′-CTTCGCCTCTGTGTGCCTAGGT-3′) [26,27]. The 50 µL PCR system contained 1 µL template DNA, 1 µL of each primer, 22 µL sterile deionized water, and 25 µL 2× Taq Plus Master Mix with dye (Vazyme Biotech, Nanjing, China). Amplification was run on a SimpliAmp™ thermal cycler (Thermo Fisher Scientific, Waltham, MA, USA) under the following thermal profile: initial denaturation at 95 °C for 5 min; 30 cycles of 95 °C (30 s), 55 °C (30 s), 72 °C (2 min); final extension at 72 °C for 10 min.

PCR amplicons were purified with the TIANGel Midi Purification Kit (Tiangen Biotech, Beijing, China), then ligated into the *pClone*007 universal vector using a cloning kit from Tsingke Biotechnology (Beijing, China). Recombinant plasmids were transformed into Escherichia coli Trelief™ 5α competent cells and cultured at 37 °C for 12–14 h. Positive clones carrying target inserts were bidirectionally sequenced with vector universal primers M13F (5′-TGTAAAACGACGGCCAGT-3′) and M13R (5′-CAGGAAACAGCTATGACC-3′). Sequencing was completed by Tianyi Huayu Gene Technology (Wuhan, China).

2.4. Sequence Alignment, Phylogenetic Tree Construction ITS Secondary Structure Prediction

Obtained cyanobacterial 16S–23S rRNA sequences were subjected to BLASTn searches against the NCBI online database. High-quality reference sequences were downloaded from GenBank for phylogenetic reconstruction. Sequence alignment and trimming were conducted in MAFFT v7.463, followed by manual refinement in BioEdit v7.0.9 [28,29]. *Gloeobacter violaceus* was selected as the outgroup taxon for constructing the full-length 16S rRNA phylogenetic tree. Multiple sequence alignment was performed to generate a dataset consisting of 101 16S rRNA sequences spanning 1192 nucleotide positions. The optimal nucleotide substitution model was screened via the ModelFinder plugin within PhyloSuite v1.2.3 [30].

Maximum likelihood (ML) and Bayesian inference (BI) trees were separately built using IQ-TREE v2.1.3 and MrBayes v3.2.7 [31,32]. The TIM3+F+I+R3 model was selected for ML inference under the Akaike information criterion (AIC), while the GTR+F+I+G4 model was adopted for BI under the Bayesian information criterion (BIC). ML bootstrap

support was assessed with 1000 replicates. For BI analyses, Markov Chain Monte Carlo (MCMC) chains ran for 10,000,000 generations with sampling every 100 generations; the initial 25% samples were discarded as burn-in, and convergence was confirmed when the average standard deviation of split frequencies dropped below 0.01. A neighbor-joining (NJ) tree with 1000 bootstrap replicates was constructed in MEGA v11 based on the maximum composite likelihood model [33]. All phylogenetic trees were visualized and annotated in FigTree v1.4.3 and further detailed in Adobe Illustrator 2022. (http://tree.bio.ed.ac.uk/software/figtree/, accessed on 6 June 2026) [34]. Pairwise p-distance calculations based on the Kimura 2-parameter model were performed in MEGA v11 to generate the sequence similarity matrix [33]. Molecular phylogenetic analyses of 16S rRNA sequences were implemented to clarify the evolutionary affinities among the sessile cyanobacterial strains isolated in the present study.

2.5. ITS Secondary Structure Prediction

Prior to secondary structure prediction of the 16S–23S ITS region, embedded tRNA genes were identified and validated via the web-based platform tRNAscan-SE 2.0.9. The boundaries of ITS subregions were then delimited according to the locations of annotated tRNA genes and previously defined molecular markers [35]. The nucleotide sequences of three key helical domains (D1–D1′, Box-B, and V3) were submitted to the RNAfold web server (http://rna.tbi.univie.ac.at/cgi-bin/RNAWebSuite/RNAfold.cgi, accessed on 6 June 2026) for secondary structure prediction, with all calculation parameters set to default values. Predicted ITS secondary structure diagrams were finally visualized and graphically refined using Adobe Illustrator 2022 [36].

3. Results

3.1. Morphological Description

Microcoleus wenzhouensis Y. Cheng, Y. Wu et R. Li sp. nov. (Figure 2).

Diagnosis: Morphologically, this strain resembles members of *Microcoleus* and *Phormidium*. The type species of related genera possess cylindrical filament apices, while the apical cells of the present species are either conical or cylindrical.

Description: As shown in Figure 2, in natural habitats, this species aggregates to form thick algal mats when biomass is abundant. Filaments are long, unbranched, straight or slightly curved, and generally bright green, turning distinctly yellowish-brown upon senescence. Filaments are surrounded by colorless, firm sheaths. Solitary filaments are isopolar or apically attenuate, with transverse walls that are constricted or non-constricted. Vegetative cells are commonly discoid, ranging from 1.12 to 3.33 μm in length and 4.43 to 5.18 μm in width, being consistently broader than long, and lacking conspicuous granular inclusions. Apical cells are cylindrical or conical, without thickened outer cell walls. Neither calyptrae nor gas vesicles are present. Reproduction proceeds via hormogonia.

Reference strain: WZU 2023.

Type locality: Collected from Sanyang Wetland, Zhejiang Province, China (October 2023, 120°43′ E, 29°57′ N).

Holotype here designated: Dry material of this strain WZU 2023 with No. WZUH-SYSD202323, stored at the Algae Culture Collection of the College of Life and Environmental Science at Wenzhou University in Wenzhou, China Academy of Science, Wuhan, Hubei Province, China.

Etymology: The species name '*wenzhouensis*' was chosen because this strain was separated from Wenzhou city.

Habitat: Epilithic on riparian rocks.

Kamptonema schistus Y. Cheng, Y. Wu et R. Li sp. nov. (Figure 3):

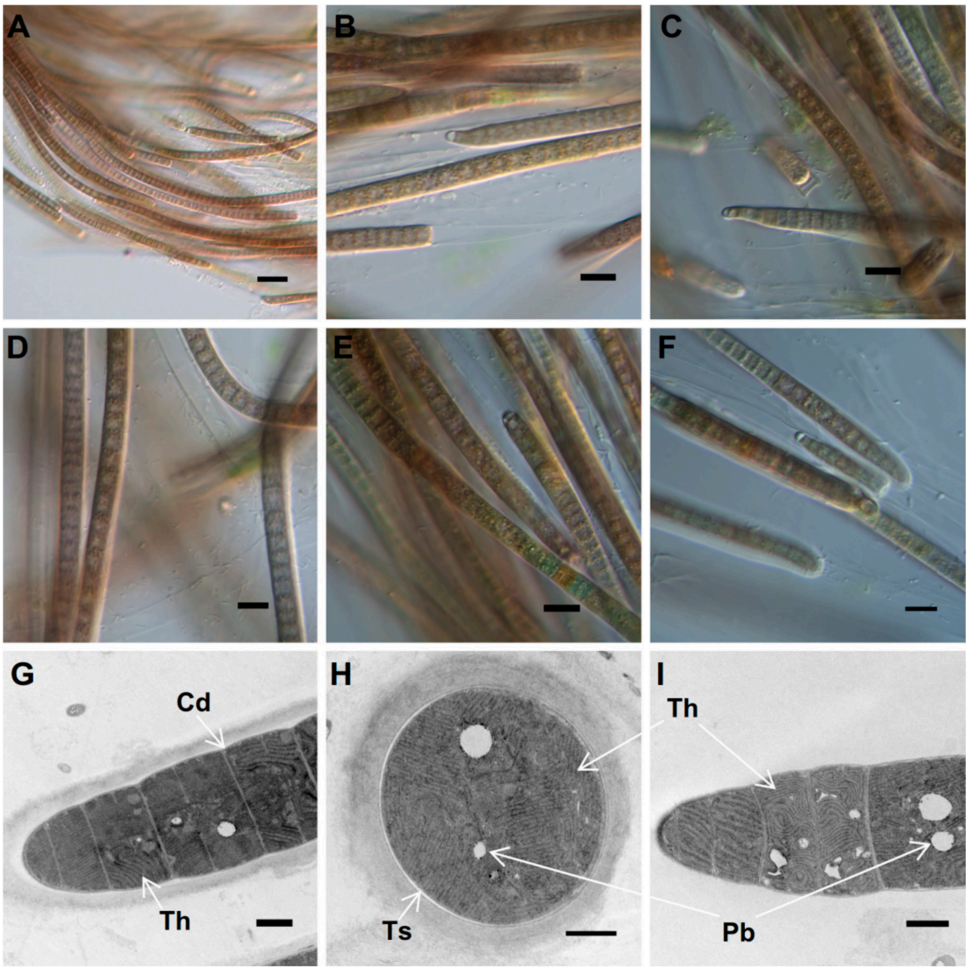


Figure 2. Light microscopy of *Microcoleus wenzhouensis* strain (**A**–**F**). Ultrastructure of *Microcoleus wenzhouensis* strain. (Cd, cell division—formation of new cell wall; Th, thylakoids; Pb, Phycobiliprotein) (**G**,**I**). Ts, Transverse section (**H**). Longitudinal sections. Scale bars: (**A**) = 20 μm, (**B**–**F**) = 10 μm, (**G**,**I**) = 5 μm, (**H**) = 2 μm.

Diagnosis: Filaments are usually solitary and sheathless. Filaments are simple, cylindrical, isopolar or attenuate, and pale blue-green in color; they turn yellowish-green during senescence under laboratory culture conditions. Transverse walls are slightly constricted or non-constricted. Vegetative cells are isodiametric, slightly longer or shorter than broad. Apical cells are rounded, occasionally curved, and devoid of calyptra. The terminal two to three cells are frequently bent or folded along the longitudinal axis.

Description: Benthic cyanobacteria typically attach to rocks along freshwater riverbanks, where they can form thin algal mats when biomass is sufficiently high. The filaments are blue-green and turn yellowish-green upon senescence (As shown in Figure 3). They usually occur singly and rarely become entangled, with apices occasionally exhibiting a slight curvature. No distinct sheaths or branches are present. The filaments are straight or slightly flexuous, with both ends tapering slightly. Vegetative cells measure 3.1–6.1 μm in length and 2.3–4.4 μm in breadth, and they are longer than or equal to their width. The cells are generally cylindrical and lack calyptrae; apical cells are either rounded or narrowed and vary in size relative to vegetative cells. The transverse walls are slightly to distinctly constricted, with granular materials present at the septa. Cell contents are uniformly distributed, and no gas vesicles are detected. Reproduction occurs via motile hormogonia formed through filament fragmentation.

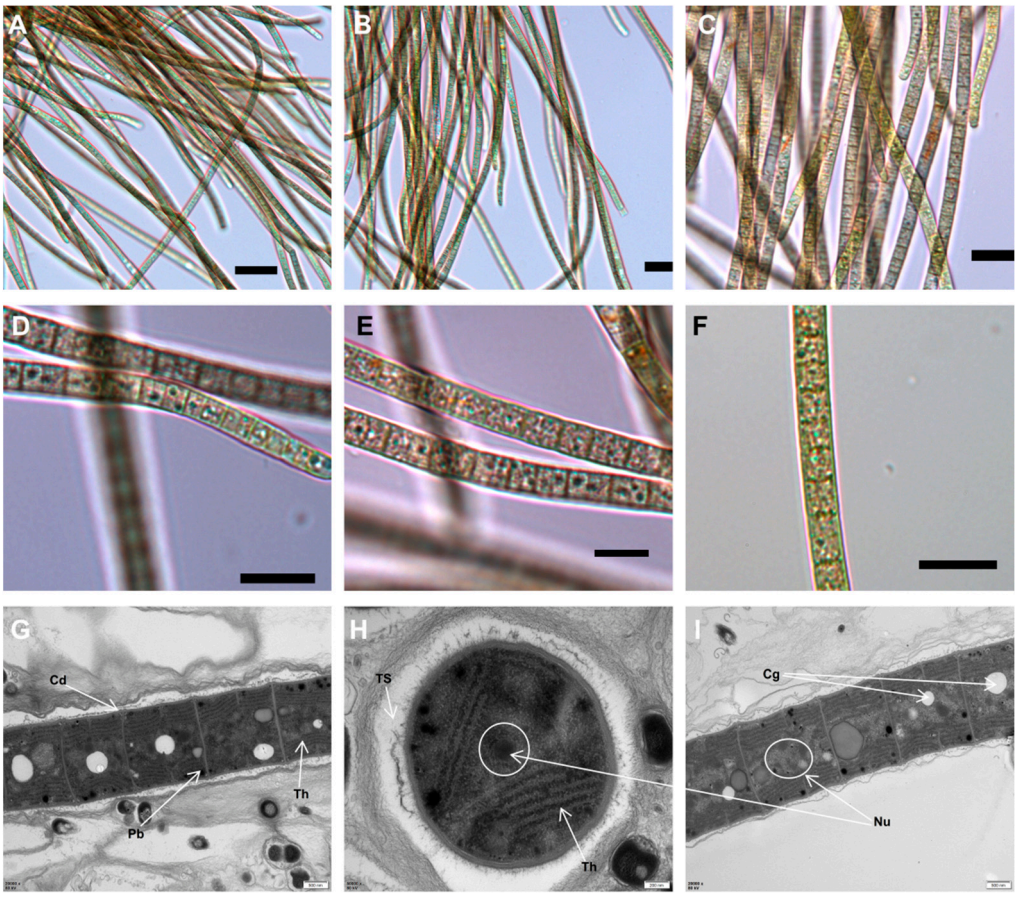


Figure 3. Light microscopy of *Kamptonema schistus* strain (**A**–**F**). Ultrastructure of *Kamptonema schistus* strain. (Cd, cell division—formation of new cell wall; Th, thylakoids; Cg, cyanophycin granules; Nu, nuclear region; Pb, Phycobiliprotein) (**G**,**I**);TS, Transverse section (**H**). Longitudinal sections. Scale bars: (**A**,**B**) = 20 µm, (**C**–**F**) = 10 µm, (**G**–**I**) = 5 µm, and (**H**) = 2 µm.

Reference strain: WZU 2025.

Type locality: Collected from Sanyang Wetland, Zhejiang Province, China (October 2023; 120°43′ E, 29°57′ N).

Holotype here designated: Dry material of this strain WZU 2025 with No. WZUH-SYSD202325, stored at the Algae Culture Collection of the College of Life and Environmental Science at Wenzhou University in Wenzhou, China Academy of Science, Wuhan, Hubei Province, China.

Etymology: The specific epithet "*schistus*" is chosen because this species was collected on rocks along the riverbank, and the Latin term "*schistus*" refers to "*schist*" (a type of rock).

Habitat: Epilithic on riparian rocks.

Wilmottia sanyangensis Y. Cheng, Y. Wu et R. Li sp. nov. (Figure 4):

Diagnosis: Trichomes are blue to dark green and grow in tightly intertwined masses with gliding motility between filaments. Trichomes are enclosed by thin, rigid, colorless sheaths; cross-walls exhibit slight constrictions. Apical cells may taper gradually or remain unattenuated. Vegetative cells are shorter than wide or isodiametric, filled with uniformly distributed dense granular cytoplasmic contents.

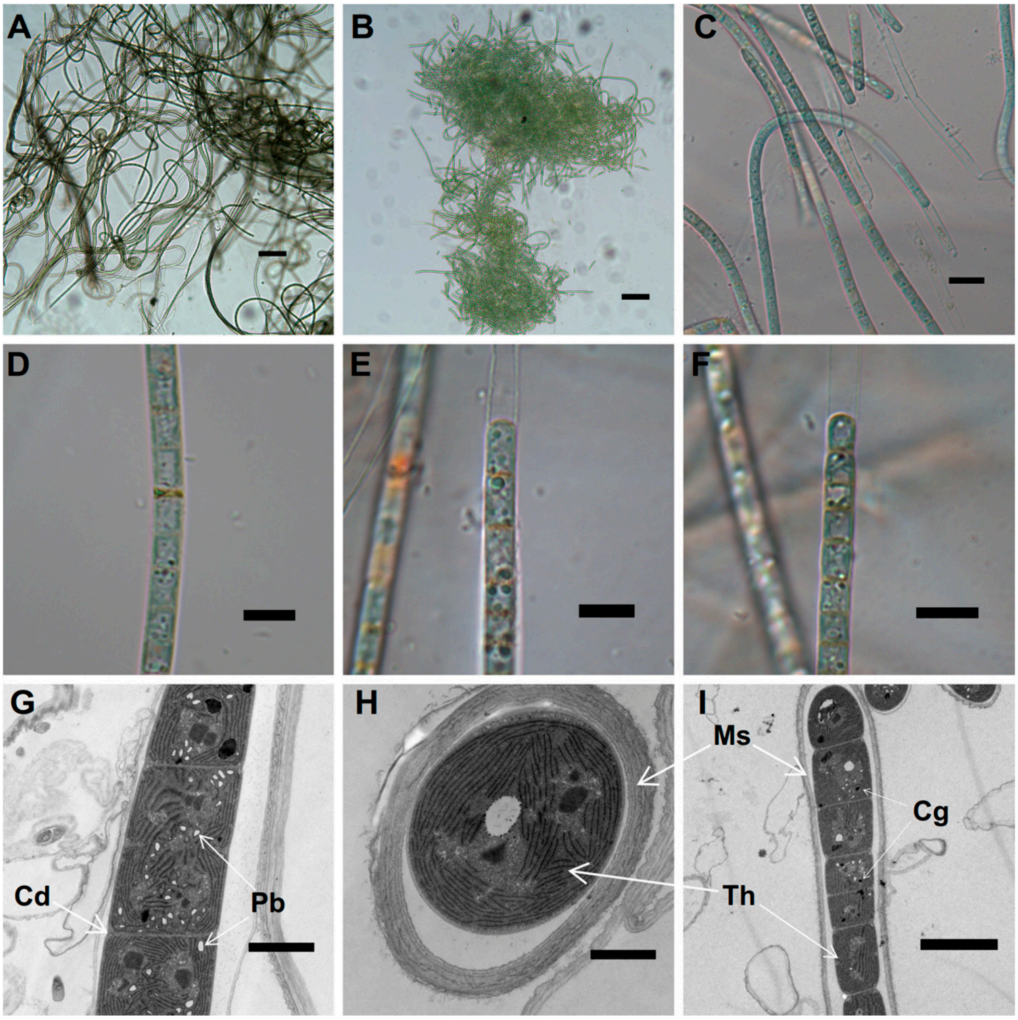


Figure 4. Light microscopy of *Wilmottia sanyangensis* strain (**A**–**F**). Ultrastructure of *Wilmottia sanyangensis* strain. (Cd, cell division—formation of new cell wall; Cg, cyanophycin granules; Th, thylakoids; Ms, Microplasmodesmata; Pb, Phycobiliprotein) (**G**–**I**). Longitudinal sections. Scale bars: (**A**) = 20 μm, (**B**–**F**) = 10 μm, (**G**,**I**) = 5 μm.

Description: Trichomes possess a simple structure and sometimes adhere to each other. They are cylindrical along their length and possess pale blue-green apical regions. Transverse walls exhibit slight to distinct constrictions, and granular materials occur at the septa (As shown in Figure 4). Vegetative cells are cylindrical, isodiametric or longer than wide, with evenly distributed cytoplasm showing weak irregular aggregation; obvious intracellular granules can be found, whereas gas vesicles are absent. Apical cells are rounded or slightly conical and lack calyptrae. Every cell is capable of division. For the investigated strains, trichomes are 6.8–10.2 μm wide, and vegetative cells range from 4.5 to 7.8 μm in length. Reproduction is realized through motile hormogonia formed by trichome fragmentation.

Reference strain: WZU 2030.

Type locality: Collected from Sanyang Wetland, Zhejiang Province, China (October 2023; 120°43′ E, 29°57′ N).

Holotype here designated: Dry material of this strain WZU 2025 with No. WZUH-SYSD202330, stored at the Algae Culture Collection of the College of Life and Environmental Science at Wenzhou University in Wenzhou, China Academy of Science, Wuhan, Hubei Province, China.

Etymology: The species name '*sanyangensis*' was chosen because this strain was separated from the Sanyang Wetland.

Habitat: Epilithic on riparian rocks.

3.2. Molecular and Phylogenetic Analyses

16S rRNA phylogenetic trees were constructed using the Neighbor-Joining (NJ), Maximum Likelihood (ML), and Bayesian Inference (BI) methods. The dataset comprised 101 sequences representing multiple taxa of Microcoleaceae and several strains of Coleofasciculaceae (Figure 5). The topological structures of the three trees were highly consistent, with no significant conflicts among branches.

The three sequences of *Microcoleus wenzhouensis* (strain WZU2023) formed a monophyletic clade with robust support, nested within the *Microcoleus* lineage, and clustered closely with multiple reference strains of *Microcoleus vaginatus* and *Microcoleus pseudautumnalis*. This novel taxon constitutes a distinct sister branch relative to known *Microcoleus* species. Similarly, the three sequences of *Kamptonema schistus* (strain WZU2025) reliably grouped with the type species *Kamptonema animale*. The two taxa formed a well-supported subclade; however, our new species occupies an independent phylogenetic branch that is clearly separated from *K. animale.* Both novel lineages are embedded within the Microcoleaceae clade, demonstrating significant phylogenetic divergence from all previously published congeners.

Within the well-supported clade corresponding to the family Coleofasciculaceae, three sequences of *Wilmottia sanyangensis* (strain WZU 2030) formed a distinct monophyletic subclade with full nodal support (bootstrap value of BI = 1). This novel taxon clustered closely with reference strains of *Wilmottia*, including *W. stricta*, *W. murrayi*, and *W. koreana*; however, it formed an independent, well-separated sister branch to all known valid *Wilmottia* species. Two sequences of the newly proposed genus and species *Paludothrix granulosa* also fell within the Coleofasciculaceae group. This lineage exhibited significant genetic divergence from all previously described genera within this family, such as *Wilmottia*, *Crustifilum*, *Coleofasciculus*, and *Anagnostidinema*. It occupied a separate phylogenetic branch that is basal to the *Lyngbya aestuarii* reference strain and showed no close affinity with any existing genus of Coleofasciculaceae, strongly supporting its establishment as a new genus. Collectively, both *Wilmottia sanyangensis* and *Paludothrix granulosa* were firmly nested within the Coleofasciculaceae clade; however, each displayed clear phylogenetic segregation from their closest known relatives, providing robust molecular evidence for their definition as novel taxa.

Pairwise 16S rRNA similarities between strains *Kamptonema schistus* WZU 2025 and *Microcoleus wenzhouensis* WZU 2023 and allied Microcoleaceae taxa were calculated via p-distance (Table 1), with an inter-strain similarity of merely 95.59%. WZU 2025 showed a peak identity of 96.76% to congener *K. animale* (below the 97.5% species threshold), and shared 92.70–94.77% similarity with other Microcoleaceae genera. WZU2023 exhibited its maximum similarity (96.86%) to *Microcoleus vaginatus*, alongside 95.26–95.86% identity to other *Microcoleus* species and 95.50% to K. animale; all cross-generic similarities fell below 97.5%. Such low sequence divergence thresholds confirm the two strains as distinct novel Microcoleaceae species.

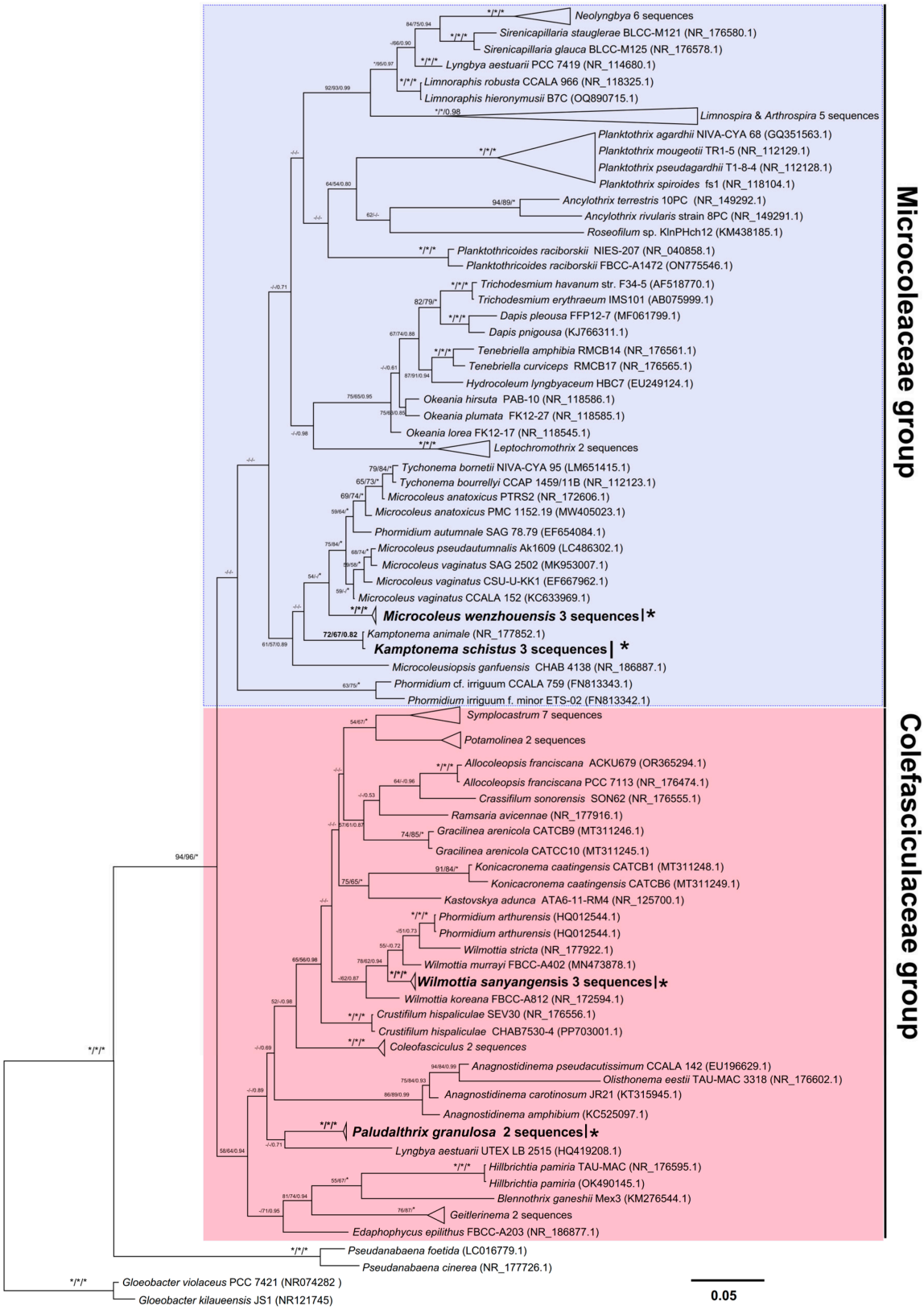


Figure 5. The phylogenetic tree of Microcoleaceae and Coleofasciculaceae and outgroup strains was constructed using the maximum likelihood (ML) approach based on 16S rRNA gene sequences. On the BI tree, bootstrapping values exceeding 50% are displayed for both NJ and ML methods, along with Bayesian posterior probabilities. Asterisks (*) denote bootstrapping values of 100 in the ML analysis, NJ method, and BI posterior probabilities of 1.00. The new filamentous strains identified in this research are highlighted in bold.

Table 1. Comparison of the 16S rRNA gene sequence similarity between Microcoleaceae WZU strains and closely related species. Similarity = [1 − (p-distance)] × 100.

Strains	GenBank	1	2	3	4	5	6	7	8	9	10
1. *Kamptonema schistus* WZU2025	PZ783778	-	-	-	-	-	-	-	-	-	-
2. *Microcoleus wenzhouensis* WZU2023	PZ782711	95.59	-	-	-	-	-	-	-	-	-
3. *Kamptonema animale* CCALA139	EF654054	96.76	95.50	-	-	-	-	-	-	-	-
4. *Microcoleus acremannii* CPCC313	NR186902	93.40	95.26	94.76	-	-	-	-	-	-	-
5. *Microcoleus antarcticus* CPCC 474	OL310652	93.33	95.86	94.59	97.67	-	-	-	-	-	-
6. *Microcoleus rushforthii* UTCC:296	OR365294	92.70	95.32	94.59	98.16	98.11	-	-	-	-	-
7. *Microcoleus vaginatus* CSU-U-KK1	NR176474	94.77	96.86	95.68	98.56	97.12	96.67	-	-	-	-
8. *Microcoleusiopsis ganfuensis* CHAB4138	NR172594	93.78	95.33	94.33	93.42	93.26	93.44	95.06	-	-	-
9. *Tychonema bourrellyi* CCAP1459	MZ700337	93.87	96.41	95.59	97.39	97.93	98.83	97.75	94.43	-	-
10. *Microcoleus anatoxicus* PTRS2	MF581657	94.05	96.68	95.77	97.39	97.84	98.38	98.20	94.43	99.55	-

Similarly, pairwise 16S rRNA sequence similarities of *Wilmottia sanyangensis* WZU2030 were calculated via p-distance correction (Table 2). The strain exhibited maximum identity of 96.65% to *Wilmottia murrayi* FBCC-A402, followed by 95.73% to *W. stricta* 31PC and 95.56% to two *W. koreana* strains (WZU0140, FBCC-A812). Its similarity to the misclassified strain "*Phormidium arthurensis*" reached 97.16%. All pairwise identities between WZU 2030 and valid *Wilmottia* species were lower than the 97.5% species-delimitation threshold, providing molecular evidence supporting its establishment as a novel species of *Wilmottia*.

Table 2. Comparison of the 16S rRNA gene sequence similarity between WZU 2030 and closely related species. Similarity = [1 − (p-distance)] × 100.

Strains	GenBank	1	2	3	4	5
1. *Wilmottia sanyangensis* WZU2030	PZ783778	-	-	-	-	-
2. *Wilmottia koreana* WZU0140	-	95.56				
3. *Wilmottia koreana* FBCC-A812	NR172594	95.56	98.56			
4. *Wilmottia_stricta* 31PC	NR177922	95.73	95.73	95.15		
5. *Wilmottia murrayi* FBCC-A402	MN473878	96.65	96.65	96.59	95.94	
6. "*Phormidium arthurensis*"	HQ012544	97.16	97.26	96.71	97.01	96.29

3.3. Molecular Analyses on the ITS Between 16S and 23S rRNA Genes

Partial 16S–23S internal transcribed spacer (ITS) sequences of *K. schistus* WZU 2025 and *M. wenzhouensis* WZU 2023 were obtained, with total lengths of 761 bp and 641 bp, respectively (Table 2). For comparative analysis, ITS sequences of *K. animale* CCALA 139, *M. vaginatus* CSUUKK1, *M. ganfuensis* CHAB 4138, and *M. anatoxicus* PTRS2 were retrieved from the NCBI database. The secondary structures of the ITS regions were predicted and constructed (Figures 6–8), and the lengths of the complete ITS and key helical regions were measured (Table 3). Partial 16S–23S ITS sequences of *Wilmottia sanyangensis* WZU2030 were obtained with a total length of 465 bp (Table 4). For comparative analysis, ITS sequences of four related Wilmottia strains (*W. koreana* WZU 0140, *W. koreana* FBCC-A812, *W. stricta* 31PC, *W. murrayi* FBCC-A402) were downloaded from NCBI. Secondary structures of ITS spacers were predicted, and nucleotide lengths of the complete ITS and characteristic helical domains were quantified (Table 4).

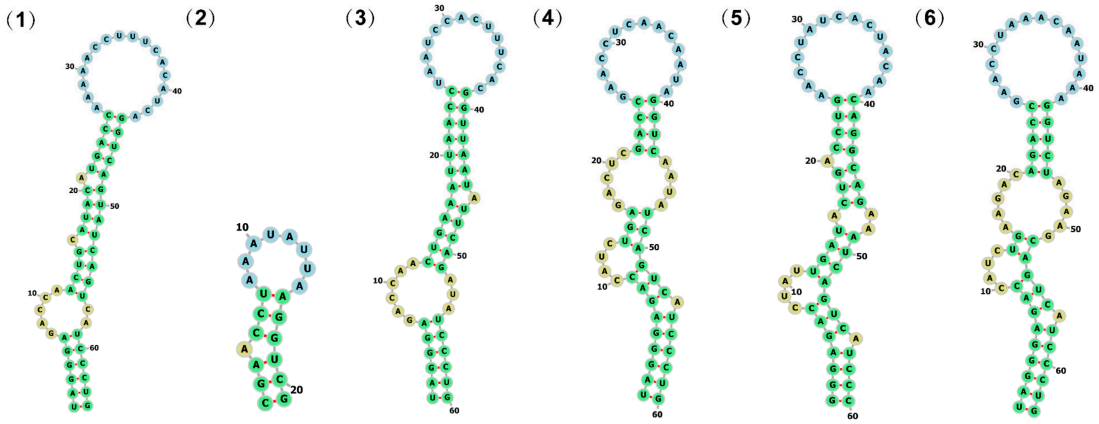


Figure 6. Secondary structures of the D1–D1′ helix in close *Kamptonema schistus* WZU2025 and *Microcoleus wenzhouensis* WZU2023. (**1**–**6**) D1–D1′ helices: (1) *Kamptonema schistus* WZU2025. (**2**) *Microcoleusiopsis sanyangensis* WZU2023. (**3**) *Kamptonema animale* CCALA139. (**4**) *Microcoleus vaginatus* CSU-U-KK1. (**5**) *Microcoleusiopsis ganfuensis* CHAB4138. (**6**) *Microcoleus anatoxicus* PTRS2. In the secondary structure diagram of simulated folding, the ring structure is shown in blue, the stem structure is shown in green, and the bilateral bulges are shown in yellow.

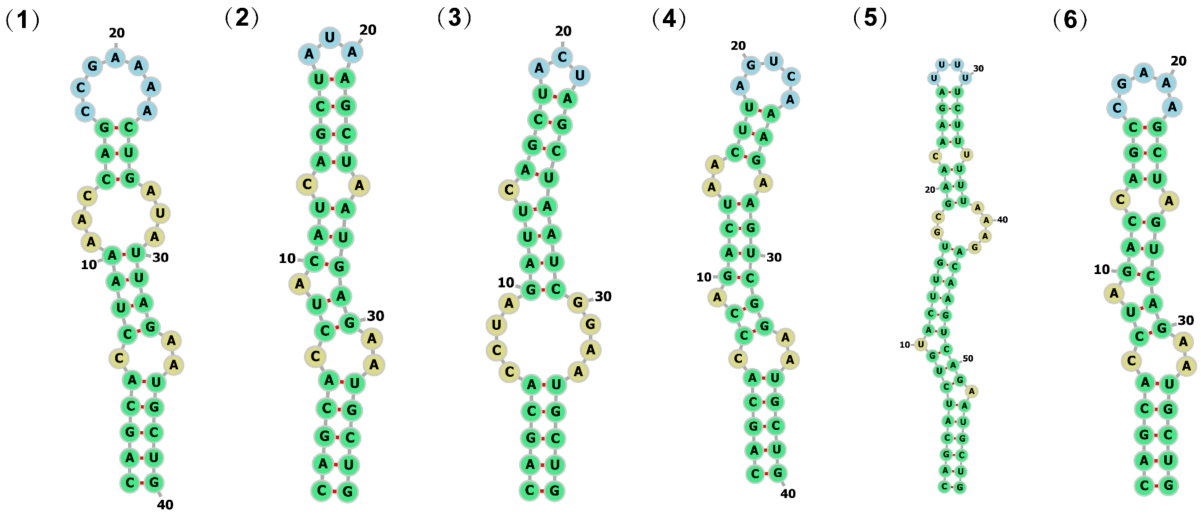


Figure 7. Secondary structures of the Box-B helix in close *Kamptonema schistus* WZU 2025 and *Microcoleus wenzhouensis* WZU 2023. (**1**–**6**) Box-B helices: (**1**) *Kamptonema schistus* WZU 2025. (**2**) *Microcoleusiopsis sanyangensis* WZU 2023. (**3**) *Kamptonema animale* CCALA139. (**4**) Microcoleus vaginatus CSU-U-KK1. (**5**) *Microcoleusiopsis ganfuensis* CHAB4138. (**6**) *Microcoleus anatoxicus* PTRS2. In the secondary structure diagram of simulated folding, the ring structure is shown in blue, the stem structure is shown in green, and the bilateral bulges are shown in yellow.

The D1–D1′ helix of WZU 2025 differed from that of *K. animale*. While both shared a 6 bp basal stem, their bilateral bulges differed (5:2 bp in WZU 2025 vs. 6:3 bp in *K. animale*), accompanied by nucleotide variations. WZU2025 contained two 1 bp unilateral bulges, whereas *K. animale* had one. The apical loop of WZU2025 was 18 nt, longer than the 16 nt loop of *K. animale* (Figure 6).

In the BoxB helix, WZU 2025 had two bilateral bulges (1:2, 3:3), while *K. animale* had one bilateral bulge (4:4) plus one unilateral bulge. The basal loop regions differed structurally and in sequence. The apical loop of WZU2025 was 7 nt, compared with 3 nt in K. animale (Figure 5). The V3 helix also differed: WZU2025 had 2:2 and 2:1 bilateral bulges and a 7 nt apical loop, while *K. animale* had 1:1 and 2:3 bilateral bulges and a 4 nt apical loop (Figure 7).

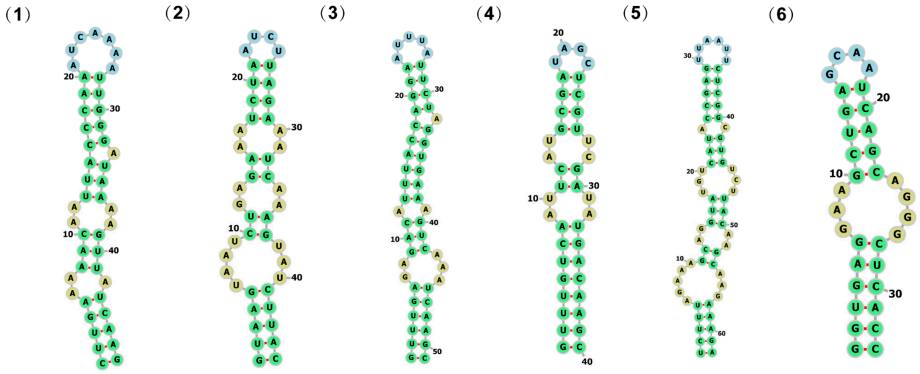


Figure 8. Secondary structures of the V3 helix in close *Kamptonema schistus* WZU 2025 and *Microcoleus wenzhouensis* WZU 2023. (**1**–**6**) V3 helices: (**1**) *Kamptonema schistus* WZU2025. (**2**) *Microcoleusiopsis sanyangensis* WZU 2023. (**3**) *Kamptonema animale* CCALA139. (**4**) *Microcoleus vaginatus* CSU-U-KK1. (**5**) *Microcoleusiopsis ganfuensis* CHAB4138. (**6**) *Microcoleus anatoxicus* PTRS2. In the secondary structure diagram of simulated folding, the ring structure is shown in blue, the stem structure is shown in green, and the bilateral bulges are shown in yellow.

Table 3. Analysis of the length (number of nucleotides) of the 16S-23S ITS region of close Microcoleaceae WZU strains.

Strains	Genbank	Complete ITS (nt)	D1-D1′ Helix (nt)	tRNAIle	tRNAAla	Box-B Helix (nt)	Box-A Helix (nt)	D4	V3 Helix (nt)	D5
1. *Kamptonema schistus* WZU2025	PZ783778	761	64	+	+	40	12	7	47	46
2. *Microcoleus wenzhouensis* WZU2023	PZ782711	641	21	+	+	37	12	7	45	38
3. *Kamptonema animale* CCALA139	KP221931	638	60	+	+	38	12	7	51	29
4. *Microcoleus vaginatus* CSU-U-KK1	EF667962	586	60	+	-	40	13	7	40	35
5. *Microcoleusiopsis ganfuensis* CHAB4138	OK422507	810	60	+	+	58	12	7	62	33
6. *Microcoleus anatoxicus* PTRS2	MT013209	631	63	+	+	37	12	7	33	36

Table 4. Analysis of the length (number of nucleotides) of the 16S-23S ITS region of *Wilmottia* strains.

Strains	Genbank	Complete ITS (nt)	D1-D1′ Helix (nt)	tRNAIle	tRNAAla	Box-B Helix (nt)	Box-A Helix (nt)	D4	V3 Helix (nt)	D5
1. *Wilmottia sanyangensis* WZU2030	PZ783778	388	65	+	-	31	12	7	46	11
2. *Wilmottia koreana* WZU0140	-	435	63	+	-	44	12	7	46	11
3. *Wilmottia koreana* FBCC-A812	NR172594	417	62	+	-	41	12	7	42	14
4. *Wilmottia_stricta* 31PC	NR177922	392	33	+	-	39	12	7	46	9
5. *Wilmottia murrayi* FBCC-A402	MN473878	428	66	+	-	55	12	7	67	13

For WZU 2023, the D1–D1′ helix was 21 nt, with a 3 bp basal stem and an 8 bp apical loop, containing one 1 bp unilateral bulge. This structure differed from *M. ganfuensis*, which had an additional 4 bp unilateral bulge and a 1:2 bilateral bulge. The D1–D1′ helices of *M. vaginatus* and *M. anatoxicus* were similar to each other but distinct from WZU 2023 (Figure 6). The BoxB helix of WZU 2023 shared a 1:1 bilateral bulge with *M. ganfuensis* but differed in basal stem length and apical loop shape, with more pronounced differences from *M. vaginatus* and *M. anatoxicus* (Figure 7). The V3 helix of WZU2023 shared a 4 bp apical loop with *M. vaginatus* and *M. anatoxicus* and a 4:3 bilateral bulge with *M. ganfuensis*, but differed in basal stem length and total helix length (Figure 8).

Wilmottia sanyangensis WZU 2030 differs from conspecific *Wilmottia koreana* WZU 0140 in D1–D1′ helix architecture. Though both have a 6 bp basal stem, their bilateral bulges (4:2, 5:3 bp) and nucleotides diverge. WZU 2030 has three 1 bp unilateral bulges and a

19 nt apical loop, versus one unilateral bulge and a 15 nt loop in WZU 0140. In the Box-B helix, WZU 2030 carries two bilateral bulges (2:3, 3:1), while WZU 0140 has one 3:3 bilateral bulge plus a 2 bp unilateral bulge. Their basal loop sequences and structures differ, with apical loops of 8 nt and 4 nt respectively. The V3 helices also diverge: WZU 2030 has 1:3, 2:2 bilateral bulges and an 8 nt apical loop, compared with 2:1, 1:2 bulges and a 5 nt loop in WZU 0140. Against reference strains FBCC-A812 (*W. koreana*), 31PC (*W. stricta*) and FBCC-A402 (*W. murrayi*), WZU 2030 has a 22 nt D1–D1′ helix with a 3 bp basal stem, 9 nt apical loop and one 1 bp unilateral bulge. This structure separates it from 31PC, which has extra bulges; FBCC-A812 and FBCC-A402 share similar D1–D1′ folding but differ from WZU 2030 (As shown in Figure 9).

WZU 2030's Box-B helix shares a 2:2 bilateral bulge with FBCC-A812 but differs in stem and loop features, with larger gaps versus 31 PC and FBCC-A402. Its V3 helix has a 5 nt apical loop matching 31PC/FBCC-A402 and a 3:2 bilateral bulge consistent with FBCC-A812, while basal stem and total helix lengths vary across all strains (Figure 9).

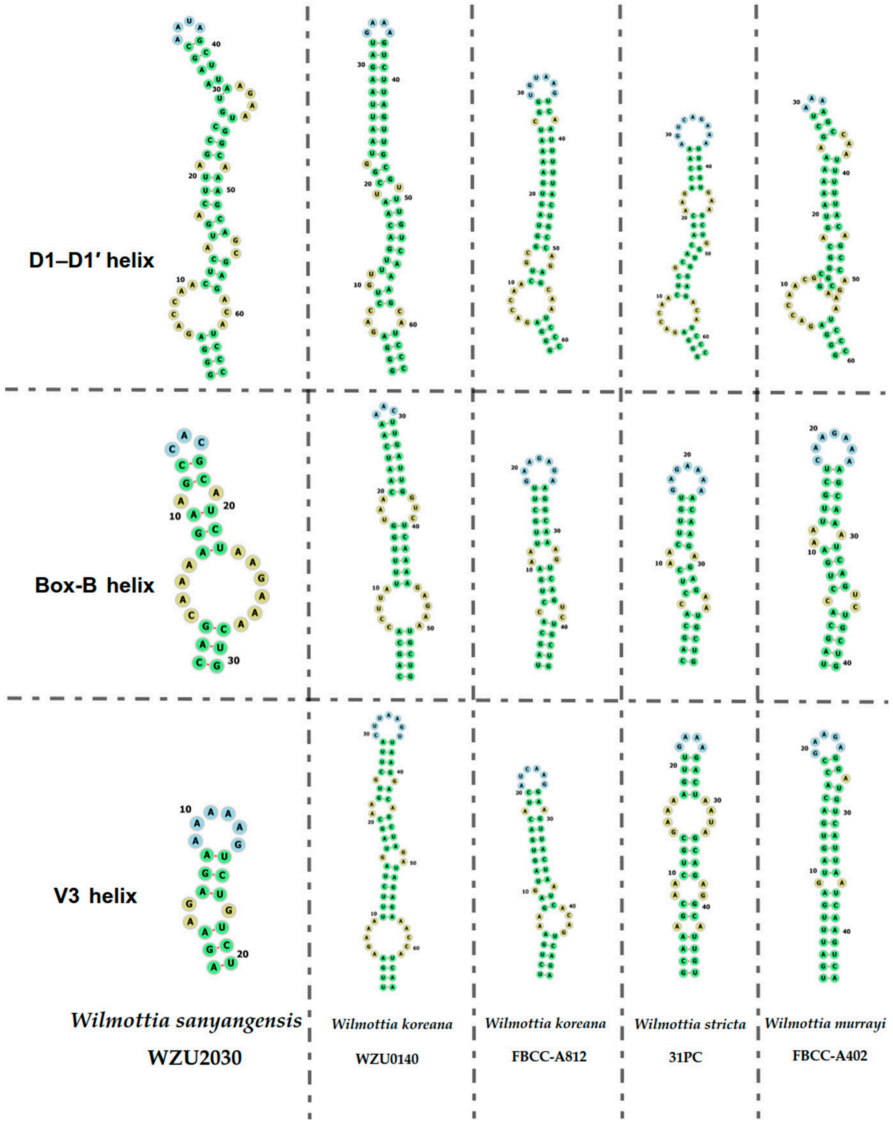


Figure 9. The D1–D1′, Box-B and V3 helix secondary structures were compared between *Wilmottia sanyangensis* WZU 2030 and other congeneric *Wilmottia* species. In the secondary structure diagram of simulated folding, the ring structure is shown in blue, the stem structure is shown in green, and the bilateral bulges are shown in yellow.

4. Discussion

Wetlands constitute critical hotspots of cyanobacterial diversity, where high habitat heterogeneity supplies diverse ecological niches. Unlike well-studied planktonic cyanobacteria, epilithic benthic cyanobacteria remain poorly classified owing to slow growth, difficult cultivation and strong phenotypic plasticity [37–40]. In this study, three filamentous strains isolated from rocks in Wenzhou Sanyang Wetland were assigned to *Kamptonema*, *Microcoleus* and *Wilmottia* via polyphasic taxonomy, expanding the known cyanobacterial diversity of wetland rocky habitats and supporting the delimitation of intergeneric boundaries [15,16,22].

The three strains isolated from Sanyang Wetland contribute to the documented diversity of epilithic filamentous cyanobacteria within the Microcoleaceae family. Morphological and molecular evidence support the establishment of three novel species associated with *Kamptonema*, *Microcoleus*, and *Wilmottia*. These taxa offer valuable material for interpreting ambiguous intergeneric boundaries within the family, which continue to pose a persistent challenge in Oscillatoriales taxonomy. In recent years, rapid advances in molecular biology have facilitated the widespread application of polyphasic taxonomy, leading to continuous revisions and improvements in the cyanobacterial classification system [41,42]. On one hand, numerous new species have been discovered and described; on the other hand, the taxonomic status of many historically recognized species has undergone constant updates and amendments [43].

Recent taxonomic revisions of the Microcoleaceae family have continuously revealed previously unrecognized generic-level diversity, exemplified by the establishment of the genus Microcoleusiopsis [23]. Morphological similarities between Microcoleusiopsis and both *Microcoleus* and *Phormidium* demonstrate that phenotypic traits alone are insufficient for reliably circumscribing genera. The strain *Microcoleus* wenzhouensis WZU 2023 shares several morphological features with the type species of *Microcoleusiopsis*, including the presence of sheaths, the absence of gas vesicles, and comparable vegetative cell dimensions. Nevertheless, clear divergence in 16S rRNA sequences and ITS structures distinguishes our strain from *Microcoleusiopsis ganfuensis*, further illustrating that morphologically similar strains may belong to phylogenetically distinct lineages. This morphological–molecular incongruence underscores the necessity of employing polyphasic approaches for accurate species delineation within the Microcoleaceae family. Continuous cyanobacterial investigations in Sanyang Wetland reveal considerable species diversity. After the publication of the novel genus *Paludothrix* from this wetland in 2024. This also constitutes an effective progress in the taxonomic investigation of the allied family Coleofasciculaceae [11]. Three new species belonging to Microcoleaceae and Coleofasciculaceae are described in this study.

The genus *Kamptonema*, belonging to the family Microcoleaceae, was initially classified within the genus *Phormidium*. Subsequent research has established that *Phormidium* is polyphyletic. Comprehensive morphological and molecular analyses have demonstrated that *Phormidium animale* significantly diverges from typical species within the *Phormidium* genus. Consequently, this formally established the new genus *Kamptonema* in 2014, thereby separating this taxon from *Phormidium*, with *Kamptonema animale* designated as the type species [22]. The genus is primarily characterized by solitary, blue-green filaments, the absence of sheaths or the presence of only thin temporary sheaths, isodiametric or subisodiametric vegetative cells, slightly constricted or non-constricted transverse walls, rounded, often hooked apical cells, and the absence of calyptrae. These morphological features are partially consistent with the new taxon described herein [14,16,23,44]. However, *Kamptonema schistus* WZU 2025 is devoid of sheaths and possesses conical apical cells, which distinctly differentiate it from all known congeners, thereby further validat-

ing its recognition as a novel species. The establishment of *Wilmottia sanyangensis* was likewise implemented via the above polyphasic approach. Morphological similarities and discrepancies were summarized from previously published records, and comprehensive molecular evidence provided robust support for the proposal of this novel species. These findings underscore the critical role of polyphasic taxonomy in delineating new genera and species of cyanobacteria and illustrate that the species and generic diversity within the Microcoleaceae and Coleofasciculaceae family remains substantially underestimated.

Traditional genus delimitation based solely on morphological observations necessitates continuous revision and supplementation with molecular evidence. In this study, accurate taxonomic identification of epilithic filamentous cyanobacteria from Sanyang Wetland could not be achieved by relying exclusively on morphological indicators such as cell shape, filament morphology, and sheath characteristics. This highlights the limitations imposed by morphological convergence and phenotypic plasticity in filamentous cyanobacterial classification [12,13]. Conversely, the polyphasic approach facilitates a reliable clarification of taxonomic status and phylogenetic relationships among newly discovered filamentous cyanobacteria, serving as an effective strategy to address taxonomic challenges within closely related lineages.

The 16S rRNA phylogenetic tree revealed significant intermingling among certain species of Oscillatoriaceae and Microcoleaceae. For example, *Oscillatoria acuminata*, *Oxynema aestuarii*, and *Oxynema thaianum*, which are conventionally classified within Oscillatoriaceae, did not cluster with other Oscillatoriaceae taxa [14,21]. Instead, they formed a stable composite clade with genera from Microcoleaceae, such as *Planktothrix* and *Ancylothrix*. Furthermore, *Oscillatoria amoena* and *Oscillatoria nigroviridis* were nested within the *Microcoleus* clade, indicating a close affinity with the type species, *M. vaginatus* [15,18,45]. A similar ambiguity is observed within Microcoleaceae: traditionally classified species such as *Microcoleus paludosus*, *M. steenstrupii*, and *M. glaciei* did not group with *M. vaginatus*, but instead formed well-supported independent lineages that are distantly related to typical *Microcoleus*. These phenomena illustrate that the current taxonomic assignments of many Oscillatoriaceae and Microcoleaceae species are ambiguous, as traditional morphology-based classifications are inconsistent with molecular phylogenetic data. This inconsistency necessitates a re-evaluation and revision of taxonomic classifications using multi-evidence data.

The family Coleofasciculaceae, described in this study, represents a significant taxonomic revision (Coleofasciculaceae was segregated from Microcoleaceae) proposed in recent years. Phylogenetically, *Microcoleus chthonoplastes* deviates markedly from the type genus of Microcoleaceae, and its morphological traits also differ significantly from traditional *Microcoleus* species. Based on its characteristic bundles of multiple filaments enclosed within a common sheath, Siegesmund et al. established the genus Coleofasciculus in 2008, designating the newly combined species Coleofasciculus chthonoplastes as its type species [14]. In the updated cyanobacterial classification system published by Komárek et al. in 2014, multiple genera exhibiting close phylogenetic affinity to Coleofasciculus, distant phylogenetic relationships to other families, and consistent morphological features with this genus were grouped into the newly erected family Coleofasciculaceae, with *Coleofasciculus* assigned as the type genus [12–15]. Currently, Coleofasciculaceae serves as a model family within the order Oscillatoriales. All genera in this family form well-supported monophyletic lineages at the genus level and cluster compactly on phylogenetic trees at the family level, except for *Geitlerinema* and *Roseofilum*, whose taxonomic placements remain unresolved. The genus Wilmottia, which accommodates *Wilmottia sanyangensis* WZU 2030, represents one of the most speciose genera within Coleofasciculaceae with abundant available taxonomic data [46]. The results and analyses of the present study strongly support

the establishment of *W. sanyangensis*. Large intraspecific divergence was observed in 16S rRNA gene sequence similarities across the genus, and the ITS secondary structure folding conformation of *W. sanyangensis* is uniquely distinct among all congeners.

Cyanobacterial taxonomy remains challenging, especially for filamentous taxa with high morphological resemblance and extensive phenotypic plasticity [47,48]. Traditional morphology and partial molecular data often fail to resolve species and generic boundaries. Although systematic research on Microcoleaceae has progressed, many taxonomic ambiguities remain. Genomic analyses reveal continuous variation among *Microcoleus* species, including at least 12 distinct taxa with different degrees of gene flow and genetic differentiation. Morphological adaptation correlates with genomic divergence, offering clues to revise and delimit the Microcoleaceae. Integrating genomic information and adaptive morphological features will help build a more natural classification system. Ongoing improvements to polyphasic approaches and genomic tools will further refine cyanobacterial taxonomy and advance diversity research [49,50].

5. Conclusions

Based on morphological traits, 16S rRNA sequences and ITS secondary structures, *K. schistus* WZU 2025, *Microcoleus wenzhouensis* WZU 2023 and *Wilmottia sanyangensis* WZU 2030 display consistent distinguishing features compared with known congeners. Multiple lines of evidence support the establishment of these three novel species within *Kamptonema*, *Microcoleus* and *Wilmottia*. These successive taxonomic findings demonstrate that Sanyang Wetland, a typical urban wetland with heterogeneous microhabitats, harbors greatly understudied cyanobacterial diversity, particularly epilithic filamentous cyanobacteria. Further systematic sampling and taxonomic research are necessary to comprehensively explore the wetland's cyanobacterial resources.

Author Contributions: Conceptualization, Y.F. and Y.C.; methodology, Y.C.; software, Y.C. and Y.W.; formal analysis, S.Z. and H.Z.; investigation, J.Z. and Y.C.; resources, Y.F. and H.Z.; data curation, Y.C.; writing—original draft preparation, Y.W. and Y.C.; writing—review and editing, Y.F. and R.L.; visualization, B.Z.; funding acquisition, R.L. All authors have read and agreed to the published version of the manuscript.

Funding: This study was funded by the project proposal of the National Key R&D Program of China (2025YFE0116400) and Zhejiang Provincial Natural Science Foundation of China (no. LMS26C030003) and NSFC project (NSFC 32371634).

Institutional Review Board Statement: Not applicable.

Informed Consent Statement: Not applicable.

Data Availability Statement: The 16S rRNA and ITS gene sequences are currently being deposited in the GenBank database and will be publicly accessible upon manuscript publication.

Acknowledgments: The first author thanks Zhenfei Xing for technical assistance with the TEM images, and thanks Yuting Liu for physical assistance in the process of collecting samples. All authors have read and agreed to the published version of the manuscript.

Conflicts of Interest: Author Sai Zhang was employed by the company Zhejiang Environmental Monitoring Engineering Co., Ltd. The remaining authors declare that the research was conducted in the absence of any commercial or financial relationships that could be construed as a potential conflict of interest.

References

1. Miller, R.J.; Thompson, L.M.; Garcia, S.A. Phylogenomic insights into the systematics and ecological roles of epiphytic cyanobacteria in wetlands. *Microb. Ecol.* **2023**, *45*, 123–140.
2. Zeng, X.; Zhang, H.; Zhou, B.; Liang, X.; Cui, L.; Li, H.; Qu, Y.; Luo, C. Hydrological dynamics and its impact on wetland ecological functions in the Sanjiang Plain, China. *Ecol. Indic.* **2024**, *169*, 112878. [CrossRef]
3. Ennabili, A.; Libiad, M.; Khabbach, A. Importance of Wetlands in Maintaining the Richness of Morocco's Vascular Flora. *Wetlands* **2021**, *41*, 121. [CrossRef]
4. Wang, Q.; Liu, Y.; Yu, H.; Ke, Q.; Wang, C.; Dai, C.; Zhao, M. Optical properties of chromophoric dissolved organic matter (CDOM) of water body in Sanyang wetland, China. *Desalin. Water Treat.* **2018**, *125*, 141–147. [CrossRef]
5. Kobayashi, T.; Ralph, T.J.; Sharma, P.; Mitrovic, S.M. Influence of historical inundation frequency on soil microbes (Cyanobacteria, Proteobacteria, Actinobacteria) in semi-arid floodplain wetlands. *Mar. Freshw. Res.* **2020**, *71*, 617–625.
6. Li, Z.; Zhang, H.; Wei, T.; He, L.; Wang, Y. Anoxia-adapted cyanobacteria in a marine blue hole. *Appl. Environ. Microbiol.* **2026**, *92*, e0257625. [CrossRef] [PubMed]
7. Fahad, S.; Saud, S.; Song, J.; Nawaz, T.; Zhou, R. *Cyanobacterial Blooms: Ecology, Evolution and Biogeochemical Impacts: Microbial Dynamics and Global Implications*; Springer Nature: Cham, Switzerland, 2026; pp. 25–45.
8. Cai, F.; Chen, J.; Li, S.; Li, X.; Li, R. New Taxa of Filamentous Cyanobacteria from Freshwater Habitats in China: Description of *Neoleptolyngbya* gen. nov. with Two Species, and *Pseudoleptolyngbya wuhanensis* sp. nov. *Microorganisms* **2026**, *14*, 72.
9. Shen, L.-Q.; Dai, G.; Le, Y.; Lai, S.; Liu, X.; Li, R.; Liu, J. Two new non-chlorophyll f-producing species in the Kovacikia genus (Leptolyngbyaceae, Leptolyngbyales) from the Poyang Lake Basin, China. *Front. Microbiol.* **2025**, *16*, 1578689. [CrossRef] [PubMed]
10. Geng, R.; Cheng, Y.; Chen, S.; Zhang, H.; Xiao, P.; Chen, S.; Ma, Z.; Han, B.; Li, R. *Maricoleus vaginatus* gen. et sp. nov. (Oculatellaceae, Synechococcales), a novel cyanobacterium isolated from a marine ecosystem in China. *Fottea* **2024**, *24*, 27–41. [CrossRef]
11. Wu, Y.; Cheng, Y.; Zhang, H.; Geng, R.; Xiao, P.; Cui, B.; Li, R. Discovery of a New Cyanobacterial Genus (*Paludothrix* gen. nov.) from the Sanyang Wetland in Eastern China, Reflecting the Latest Taxonomic Status in Coleofasciculaceae. *Diversity* **2025**, *17*, 15.
12. Komárek, J.; Kaštovský, J.; Mareš, J.; Johansen, J.R. Taxonomic classification of cyanoprokaryotes (cyanobacterial genera) 2014, using a polyphasic approach. *Preslia* **2014**, *86*, 295–335.
13. Strunecký, O.; Ivanova, A.P.; Mareš, J. An updated classification of cyanobacterial orders and families based on phylogenomicand polyphasic analysis. *J. Phycol.* **2022**, *59*, 12–51.
14. Siegesmund, M.A.; Johansen, J.R.; Karsten, U.; Friedl, T. *Coleofasciculus* gen. nov. (cyanobacteria): Morphological and molecular criteria for revision of the genus *Microcoleus* gomont. *J. Phycol.* **2008**, *44*, 1572–1585. [CrossRef] [PubMed]
15. Strunecký, O.; Elster, J.; Komárek, J. Taxonomic revision of the freshwater cyanobacterium "*Phormidium*" *murrayi* = *Wilmottia murrayi*. *Fottea* **2011**, *11*, 57–71. [CrossRef]
16. Strunecký, O.; Komárek, J.; Johansen, J.; Lukešová, A.; Elster, J. Molecular and morphological criteria for revision of the genus *Microcoleus* (Oscillatoriales, Cyanobacteria). *J. Phycol.* **2013**, *49*, 1167–1180. [CrossRef] [PubMed]
17. Castelo-Branco, R.; Pereira, J.P.; Freitas, S.; Preto, M.; Vieira, A.R.; Morais, J.; Leão, P.N. Genome-informed Discovery of Monchicamides A–K: Cyanobactins from the Microcoleaceae Cyanobacterium LEGE 16532. *J. Nat. Prod.* **2025**, *88*, 86–93. [CrossRef] [PubMed]
18. Guo, Z.; Wang, C.; Ji, Y.; Tang, K.; Guo, H.; Meng, J.; Ji, X.; Zhang, S. The Importance of *Microcoleus vaginatus* in Shaping Bacterial Communities Essential for the Development of Cyanobacterial Biological Soil Crusts. *Microorganisms* **2026**, *14*, 542. [CrossRef] [PubMed]
19. Xiao, J.; Lan, S.; E Farías, M.; Qian, L.; Xia, L.; Song, S.; Wu, L. The living forms of *Microcoleus vaginatus* and their contributions to the aggregate structure of biocrusts. *FEMS Microbiol. Ecol.* **2023**, *99*, 5. [CrossRef] [PubMed]
20. Hašler, P.; Dvořák, P.; Poulíčková, A.; Casamatta, D.A. A novel genus *Ammassolinea* gen. nov. (Cyanobacteria) isolated from subtropical epipelic habitats. *Fottea* **2014**, *14*, 241–248. [CrossRef]
21. Chatchawan, T.; Komárek, J.; Strunecky, O. Oxynema, a new genus separated from the genus *Phormidium* (cyanophyta). *Cryptogam. Algol.* **2012**, *33*, 41–59. [CrossRef]
22. Strunecký, O.; Komárek, J.; Šmarda, J. *Kamptonema* (Microcoleaceae, Cyanobacteria), a new genus derived from the polyphyletic *Phormidium* on the basis of combined molecular and cytomorphological markers. *Preslia* **2014**, *86*, 193–207. [CrossRef]
23. Geng, R.; Li, W.; Chao, A.; Guo, X.; Li, H.; Yu, G.; Li, R. Establishment of a New Filamentous Cyanobacterial Genus, *Microcoleusiopsis* gen. nov. (Microcoleaceae, Cyanobacteria), from Benthic Mats in Open Channel, Jiangxi Province, China. *Diversity* **2021**, *13*, 548. [CrossRef]
24. Stanier, R.Y.; Kunisawa, R.; Mandel, M.; Cohen–Bazire, G. Purification and properties of unicellular blue-green algae (order Chroococcales). *Bacteriol. Rev.* **1971**, *35*, 171–205. [CrossRef] [PubMed]

25. Neilan, B.A.; Jacobs, D.; Goodman, A.E. Genetic diversity and phylogeny of toxic cyanobacteria determined by DNA polymorphisms within the phycocyanin locus. *Appl. Environ. Microbiol.* **1995**, *61*, 3875–3883. [CrossRef] [PubMed]
26. Edwards, U.; Rogall, T.; Blöcker, H.; Emde, M.; Böttger, E.C. Isolation and direct complete nucleotide determination of entire genes. Characterization of a gene coding for 16S ribosomal RNA. *Nucleic Acids Res.* **1989**, *17*, 7843–7853. [CrossRef] [PubMed]
27. Gkelis, S.; Rajaniemi, P.; Vardaka, E.; Moustaka–gouni, M.; Lanaras, T.; Sivonen, K. *Limnothrix redekei* (Van Goor) Meffert (Cyanobacteria) strains from Lake Kastoria, Greece from a separate phylogenetic group. *Microb. Ecol.* **2005**, *49*, 176–182. [CrossRef] [PubMed]
28. Katoh, K.; Standley, D.M. MAFFT multiple sequence alignment software version 7: Improvements in performance and usability. *Mol. Biol. Evol.* **2013**, *30*, 772–780. [CrossRef] [PubMed]
29. Hall, T.A. BioEdit: A User-Friendly Biological Sequence Alignment Editor and Analysis Program for Windows 95/98/NT. *Nucleic Acids Symp. Ser.* **1999**, *41*, 95–98.
30. Zhang, D.; Gao, F.; Jakovlić, I.; Zhou, H.; Zhang, J.; Li, W.X.; Wang, G.T. PhyloSuite: An integrated and scalable desktop platform for streamlined molecular sequence data management and evolutionary phylogenetics studies. *Mol. Ecol. Resour.* **2020**, *20*, 348–355. [CrossRef] [PubMed]
31. Trifinopoulos, J.; Nguyen, L.-T.; von Haeseler, A.; Minh, B.Q. W-IQ-TREE: A fast online phylogenetic tool for maximum likelihood analysis. *Nucleic Acids Res.* **2016**, *44*, W232–W235. [CrossRef] [PubMed]
32. Ronquist, F.; Teslenko, M.; van der Mark, P.; Ayres, D.L.; Darling, A.; Höhna, S.; Huelsenbeck, J.P. MrBayes 3.2: Efficient Bayesian Phylogenetic Inference and Model Choice Across a Large Model Space. *Syst. Biol.* **2012**, *61*, 539–542. [CrossRef] [PubMed]
33. Tamura, K.; Stecher, G.; Kumar, S. MEGA11: Molecular Evolutionary Genetics Analysis Version 11. *Mol. Biol. Evol.* **2021**, *38*, 3022–3027. [CrossRef] [PubMed]
34. Page, R.D.M. TreeView: An application to display phylogenetic trees on personal computers. *Bioinformatics* **1996**, *12*, 357–358. [CrossRef] [PubMed]
35. Lowe, T.M.; Chan, P.P. tRNAscan-SE On-line: Integrating search and context for analysis of transfer RNA genes. *Nucleic Acids Res.* **2016**, *44*, W54–W57. [CrossRef] [PubMed]
36. Mathews, D.H.; Disney, M.D.; Childs, J.L.; Schroeder, S.J.; Zuker, M.; Turner, D.H. Incorporating chemical modification constraints into a dynamic programming algorithm for prediction of RNA secondary structure. *Nucleic Acids Res.* **2004**, *101*, 7287–7292. [CrossRef] [PubMed]
37. Zhao, S.; Li, B. Wetland ecosystem in Xiushan Island of Zhejiang Province. *Shengtaixue Zazhi* **2006**, *25*, 343–346.
38. Gaget, V.; Almuhtaram, H.; Kibuye, F. Benthic cyanobacteria: A utility-centred field study. *Harmful Algae* **2022**, *113*, 102185. [CrossRef] [PubMed]
39. Berthold, D.E.; Lefler, F.W.; Moretto, J.A.S.; Laughinghouse, H.D. Diversity of *Dapis* (Microcoleaceae, Cyanobacteria) from coastal marine benthic proliferations in Florida (United States) with the description of three new species. *J. Phycol.* **2025**, *61*, 1812–1826. [CrossRef] [PubMed]
40. Ubero-Pascal, N.; Aboal, M. Cyanobacteria and Macroinvertebrate Relationships in Freshwater Benthic Communities beyond Cytotoxicity. *Toxins* **2024**, *16*, 190. [CrossRef] [PubMed]
41. Sciuto, K.; Moschin, E.; Moro, I. Cryptic Cyanobacterial Diversity in the Giant Cave (Trieste, Italy): The New Genus *Timaviella* (Leptolyngbyaceae). *Cryptogam. Algol.* **2017**, *38*, 285–323. [CrossRef]
42. Cai, F.; Peng, X.; Li, R. *Violetonostoc minutum* gen. et sp. nov. (Nostocales, Cyanobacteria) from a rocky substrate in China. *Algae* **2020**, *35*, 1–15. [CrossRef]
43. Taton, A.; Grubisic, S.; Balthasart, P.; Hodgson, D.A.; Laybourn-Parry, J.; Wilmotte, A. Biogeographical distribution and ecological ranges of benthic cyanobacteria in East Antarctic lakes. *FEMS Microbiol. Ecol.* **2006**, *57*, 272–289. [CrossRef] [PubMed]
44. Palinska, K.A.; Marquardt, J. Genotypic and phenotypic analysis of strains assigned to the widespread cyanobacterial morphospecies *Phormidium autumnale* (Oscillatoriales). *Arch. Microbiol.* **2008**, *189*, 325–335. [CrossRef] [PubMed]
45. Sorokovikova, E.; Tikhonova, I.; Evseev, P.; Khanaev, I.; Krasnopeev, A.; Gutnik, D.; Fedorova, G.; Potapov, S.; Gladkikh, A.; Nebesnykh, I.; et al. *Tychonema litorale* sp. nov. (Microcoleaceae, Oscillatoriales): A New Species of Cyanobacteria Associated with Ecological Crisis in Lake Baikal Coastal Zone. *Diversity* **2026**, *18*, 84. [CrossRef]
46. Lee, N.-J.; Seo, Y.; Ki, J.-S.; Lee, O.-M. Morphology and molecular description of *Wilmottia koreana* sp. nov. (Oscillatoriales, Cyanobacteria) isolated from the Republic of Korea. *Phytotaxa* **2020**, *447*, 237–251. [CrossRef]
47. Haande, S.; Rohrlack, T.; Ballot, A.; Røberg, K.; Skulberg, R.; Beck, M.; Wiedner, C. Genetic characterisation of *Cylindrospermopsis raciborskii* (Nostocales, Cyanobacteria) isolates from Africa and Europe. *Harmful Algae* **2008**, *7*, 692–701. [CrossRef]
48. Skoupý, S.; Stanojković, A.; Casamatta, D.A.; McGovern, C.; Martinović, A.; Jaskowiec, J.; Konderlová, M.; Dodoková, V.; Mikesková, P.; JahodářOvá, E.; et al. Population genomics and morphological data bridge the centuries of cyanobacterial taxonomy along the continuum of *Microcoleus* species. *iScience* **2024**, *27*, 109444. [CrossRef] [PubMed]

49. Stanojković, A.; Skoupý, S.; Johannesson, H.; Dvořák, P. The global speciation continuum of the cyanobacterium *Microcoleus*. *Nat. Commun.* **2024**, *15*, 2122. [CrossRef] [PubMed]
50. Chen, M.-Y.; Teng, W.-K.; Zhao, L.; Hu, C.-X.; Zhou, Y.-K.; Han, B.-P.; Song, L.-R.; Shu, W.-S. Comparative genomics reveals insights into cyanobacterial evolution and habitat adaptation. *ISME J.* **2021**, *15*, 211–227. [CrossRef] [PubMed]

Disclaimer/Publisher's Note: The statements, opinions and data contained in all publications are solely those of the individual author(s) and contributor(s) and not of MDPI and/or the editor(s). MDPI and/or the editor(s) disclaim responsibility for any injury to people or property resulting from any ideas, methods, instructions or products referred to in the content.